Experimental report

15/09/2023

Proposal: 1-02-359 **Council:** 10/2022

Title: Residual stress in cemented carbides

Research area: Materials

This proposal is a new proposal

Main proposer: Elizabeth BLACKBURN

Experimental team: SHIRIN NOUHI
Anna BOHM
Juan Manuel BELLO BERMEJO
Elizabeth BLACKBURN

Local contacts: Thilo PIRLING
Sandra CABEZA

Samples: WC-Co

Instrument	Requested days	Allocated days	From	To
SALSA	6	6	02/06/2023	08/06/2023

Abstract:

We aim to examine cemented carbide composites, in this case in the form of drill buttons. These composites are hardened before use to build in compressive stresses to prevent crack propagation, but at present it is not possible find out non-destructively what happens in the bulk of the material during hardening, to identify the key components .This is of general interest to understand the mechanisms of the hardening in a composite system. We are specifically applying this to drill buttons, but the material used here is also used in the machining industry and as a potential nuclear shielding material. In addition to increasing understanding of the hardening process, this may feed back to improve device performance. To accomplish this, we plan to use SALSA to assess the residual stress in actual drill buttons.

Experimental Report
Instrument: SALSA
Experiment Number: 1-02-359

Title: Residual stress in cemented carbides

Experiment Date: 01/06/2023 – 09/06/2023

Experimental Team (on-site): Anna Böhm (Sandvik AB), Elizabeth Blackburn (Lund University)

Local Contact: Thilo Pirling

Introduction

Cemented carbides are composites of hard tungsten carbide (WC) grains in a tough binder phase based on cobalt (Co). These materials provide a unique combination of high elastic modulus, hardness, compressive strength, and wear and abrasion resistance, and have multiple uses, for example as drill buttons in mining tools, or as winter tyre studs. Tungsten has been designated a critical raw material by the European Union [1], and improving efficiency to best exploit a limited resource is important.

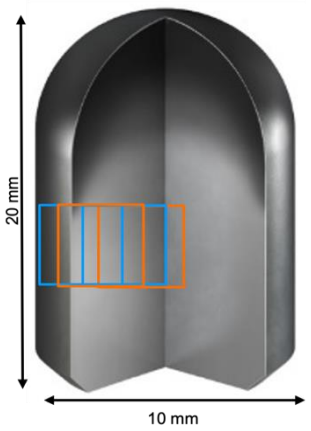

Figure 1: Sketch of the sample geometry and scanning strategy.

Our specific interest lies in their use as materials for drill buttons in mining tools (Figure 1). To minimize the risk of premature failures during use by reducing crack propagation, drill buttons are exposed to a surface hardening process after sintering, typically by vibrational tumbling. Compressive stresses are introduced through collisions between the drill buttons and tumbling media, thereby improving the fatigue resistance and fracture toughness of the final products. Figure 2a shows the residual stress (as measured by lab-XRD) near the surface of two samples, with different Co content, before (blue) and after (green) this hardening process. The residual stress near the surface is significantly more compressive after the treatment. However, we do not know if the hardening treatment has a similar effect on the bulk of the drill button.

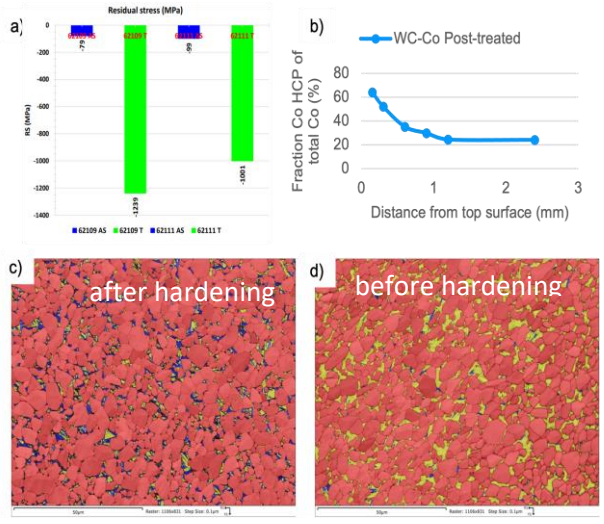

Figure 2: a): Residual stress close to the surface for two drill buttons before (blue) and after (green) post-treatment. b): Area fraction of hcp-Co as a function of distance from the surface, as measured by serial-sectioning EBSD. c)-d): EBSD phase maps of a surface region of a post-treated (c) and as-sintered (d) WC-Co drill button. WC is in red, fcc-Co in yellow, and hcp-Co in blue.

The surface zone of a post-treated drill button also shows increased strain evolution in the WC grains and phase transformations from fcc-Co to hcp-Co in the binder phase. Figures 2c and d show EBSD maps of the surface region in post-treated (c) and as-sintered (d) drill buttons. The post-treated sample contains significantly more hcp-Co (blue) than the as-sintered sample. Serial-sectioning EBSD measurements also reveal that the hcp-Co phase is mainly formed near the sample surfaces, fig. 2b). In this experiment, our

aim was to gain a better understanding of the whole sample, using what is a new method for us for examining these materials.

Sample Details and Instrumental Configurations

Three samples (11%wt. Co) were mounted, labelled (A-AS (as-sintered), A-PT (post-treatment) and B-PT). A wavelength of 2.477 Å was set using an Fe powder to calibrate. This wavelength placed both the Co(111) and WC(101) Bragg peaks at angles close to 90°. The Co(101) Bragg reflection from the hcp Co phase should then fall on the detector when measuring the WC(101) reflection, but no detectable signal was observed during the experiment. The curvature of the monochromator was also set during the calibration of the Fe powder, at 26.923°; this gave the highest figure of merit for the Fe powder signal. The primary and secondary oscillating collimators were set to give a 0.6 x 0.6 mm scan area in the horizontal plane, and the vertical size of the gauge volume was set to 2mm using a collimator just before the monochromator. In each measurement our goal was a detector count total of 3500. For the WC(101) measurements, this took ~30 minutes. For the Co(111) this took about ~45 minutes (when a signal was visible – see below).

Results

Initial measurements were done tracing out the red line shown in Figure 3. Examples of what was observed on the detector for the WC and Co measurement angles are shown in Figure 4. While the WC signal appears across the whole detector, and is of good signal strength, the Co signal does not form a continuous ring, and we think that this is due to the Co grain size relative to the gauge volume [2]. While we were able to extract information in changes to the lattice parameter for the Co, the signal strength varied arbitrarily, leading to uncertainties.

Figure 3: Initial scan line.

We therefore continued only with the WC(101) reflection, taking radial, tangential and axial measurements along the red line in Figure 3, and then measured from the top of the dome downwards in the relevant configurations (we were not able to complete all of these due to time limitations). Our results (shown in Figure 5), show a strong effect of the hardening process close to the surface. We have plotted out the results in terms of change in scattering angle. We have also converted this into lattice parameter shifts and relative strains, but include only the angular version here. The next step in our analysis is to link this in to more detailed information on the material elastic properties.

Conclusions

We have been able to monitor the lattice parameter shifts inside the samples, and can see an effect of hardening on the tungsten carbide component. To improve measurements of the Co components, rotating the sample would be one way forward to resolve the grain-size problem.

[1] European Commission, "Study on the Review of the List of Critical Raw Materials", Critical Raw Materials Factsheets (2017).
[2] K. P. Mingard *et al.*, Acta Materialia **59**, 2277 (2011).

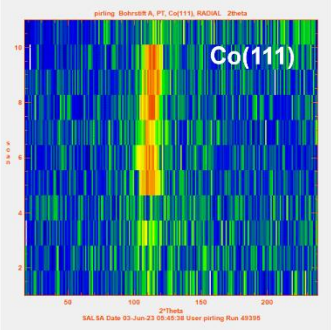

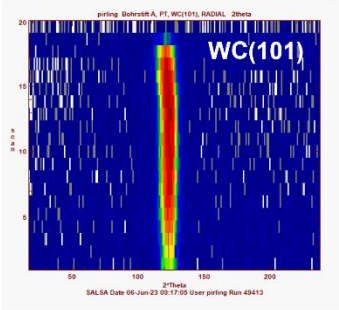

Figure 4: Raw detector output for measurements focusing on Co(111) and WC(101). The WC(101) image is as expected for a good powder-average. The Co(111) signal is typical of grains or texture.

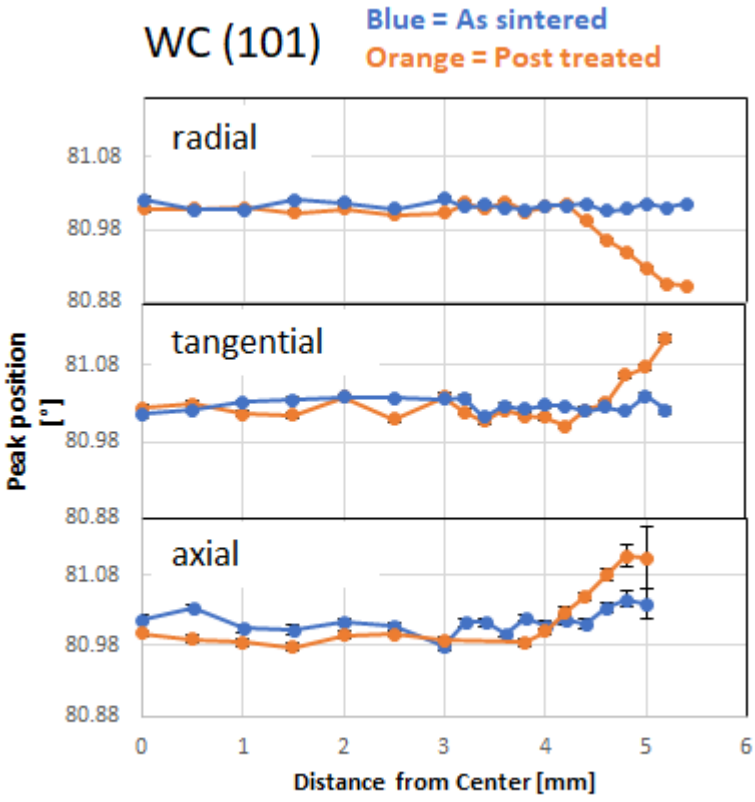

Figure 5: WC Peak center shift as a function of distance from the center of the drill bit insert. A clear change in peak position towards the sample surface can be observed in all post treated (PT) samples. Note that the errors are shown, and are typically smaller than the point size.